Desalination and Water Treatment
www.deswater.com
doi: 10.5004/dwt.2022.29055

278 (2022) 239–250
December

Fabrication of nano-activated charcoal incorporated sodium alginate-based cross-linked membrane for Rhodamine B adsorption from an aqueous solution

Sefeera Sadik Ayyaril, Muhammad Imran Khan*, Abdallah Shanableh*, Sourjya Bhattacharjee, Debora Mattos de Oliveira

Research Institute of Sciences and Engineering (RISE), University of Sharjah, Sharjah 27272, United Arab Emirates, emails: raoimranishaq@gmail.com/mimran@sharjah.ac.ae (M.I. Khan), Shanableh@sharjah.ac.ae (A. Shanableh), safeeraayyaril@sharjah.ac.ae (S.S. Ayyaril), sbhattacharjee@sharjah.ac.ae (S. Bhattacharjee), doliveira@sharjah.ac.ae (D.M. de Oliveira)

Received 30 April 2022; Accepted 18 October 2022

ABSTRACT

This work reports the fabrication of nano-activated charcoal incorporated sodium alginate-based cross-linked membrane via solution casting method. The morphology of the fabricated membrane was investigated by using scanning electron microscopy. Fourier-transform infrared spectroscopy confirmed the fabrication of the nano-activated charcoal incorporated sodium alginate-based cross-linked membrane. It presented a water uptake of 43% and was used for Rhodamine B (RhB) adsorption from an aqueous solution at room temperature. The influence of contact time, membrane dosage, and initial concentration of RhB on the percentage removal of RhB from an aqueous solution at room temperature was evaluated. At optimum conditions, a maximum percentage removal of 98% was obtained. Adsorption isotherms such as Langmuir, Freundlich, Temkin, Dubinin–Radushkevich were used to study RhB adsorption onto the fabricated membrane. Results showed that adsorption of RhB onto the fabricated nano-activated charcoal incorporated sodium alginate-based cross-linked membrane was chemical adsorption process. Adsorption kinetics were also investigated by employing kinetic models including pseudo-first-order model, pseudo-second-order model, Elovich model, liquid-film diffusion model, modified Freundlich equation and Bangham equation. Rhodamine B adsorption onto the fabricated membrane fitted to pseudo-second-order model. Therefore, the fabricated nano-activated charcoal incorporated sodium alginate-based cross-linked membrane proved efficient for RhB adsorption from an aqueous solution at room temperature.

Keywords: Rhodamine B; Fabricated cross-linked membrane; Adsorption; Chemical adsorption process; Pseudo-second-order model

1. Introduction

Dye-stuffs are organic substances, used in several industrial sectors including plastics, textile, paint, cosmetics, ink, and varnishes that result environmental pollution due to highly toxic compounds present in them [1,2]. The artificial colorants are recognized as a major source of environmental pollution, based on both the volume of dye discharged and the composition of the effluent. Resultantly, it is crucial to remove these substances from the colored effluents before being rejected to aqueous media. Rhodamine B (RhB) dye is among the mostly used dyes in the field of

* Corresponding authors.

textile and cosmetics. It is a basic dye and belongs to the group of heterocyclic organic compounds. It can cause eye burns, vomiting, cyanosis, and respiratory damage, necrosis of living tissue, nausea, tachycardia and diarrhea for humans [3]. Therefore, it is crucial to take necessary measures to minimize the effects of Rhodamine B (RhB) onto human and animals.

The removal of dyes from an aqueous solution was carried out by using physical, chemical, and biological procedures [4–6]. Adsorption is considered as an excellent procedure for dye removal among these reported procedures. It is because of higher efficiency, economic feasibility and operations and easy to design [6–12]. Therefore, it is significant to utilize an adsorbent with higher capability for the removal dyes from an aqueous solution.

Commonly utilized adsorbents that exhibited oxtraordinary capability for dye removal from an aqueous solution were demonstrated to date by researchers [7,13]. For the color removal, commonly the commercial activated carbon is an excellent adsorbent. Its large scale uses were restricted due to its higher price. Among the latest trends, mesoporous carbons are gaining fame as efficient adsorbents. Ordered metal halide free mesoporous carbons have been successfully applied for the removal of basic dyes [14]. A lot of adsorbents including walnut husk [15], composites [16], commercial anion exchange membrane [17,18], synthesized anion exchange membranes [19,20], rice husk [21], leaves powder of various plants [6,22], biochars from crop residues [23], natural clinoptilolite [24], sesame hull [25], biomass of Penicillium YWO1 [26], natural zeolite [27], cross-linked succinyl chitosan [28], modified bentonite [29], eucalyptus barks [30] modified attapulgite [31], clay material [32–34], activated carbon [35], dehydrated beet pulp carbon [36], polyurethane foam [37], etc. were employed for the removal of dyes from an aqueous solution. Similarly, metal organic frameworks have also superceded many adsorbents as efficient dye removing agents [38]. Agriculture by-products showed its efficiency as a low cost adsorbents and they were mostly being modified chemically to enhanced their adsorption capability toward the dyes [39]. Nevertheless, there are some adsorbents which represented poor adsorption capacity for the anionic dyes due to their anionic or hydrophobic surfaces. Therefore, the removal of dyes from an aqueous solution demands cheap and effective adsorbents [40]. We shall report the synthesis of low cost membrane for adsorption of RhB from an aqueous solution. To the beat of our knowledge, the fabrication of nano-activated charcoal incorporated sodium alginate-based cross-linked membrane has not been reported yet.

In this research, the fabrication of the nano-activated charcoal incorporated sodium alginate-based cross-linked membrane was reported via solution casting method for RhB removal from an aqueous solution at room temperature. The fabricated membrane was characterized in term of Fourier-transform infrared spectroscopy (FTIR), morphology, surface area and water uptake. It was used for RhB adsorption from an aqueous at room temperature. The effect of operating factors on the percentage removal of RhB from an aqueous solution was studied in detail. Adsorption isotherm and kinetics for RhB adsorption onto the fabricated membrane was revealed.

2. Experimental

2.1. Materials

Alginic acid sodium salt powder, calcium chloride dihydrate were purchased from Sigma-Aldrich (St. Louis, Missouri, United States). Nano-activated charcoal was supplied by BDH Middle East FZ LLC (Dubai, United Arab Emirates). Rhodamine B was bought from Sinopharm Chemical Reagent Co., Ltd., (Shanghai, China). Chemical structure of RhB is represented in Fig. S1. Deionized water was used throughout this work.

2.2. Fabrication of fabricated nano-activated charcoal incorporated sodium alginate-based cross-linked membrane

The fabrication of nano-activated charcoal incorporated sodium alginate-based cross-linked membrane was carried out by solution casting method as reported in our previous work [41–45]. Firstly, 1.5% activated charcoal powder was mixed with 3% sodium alginate solution. The mixture was stirred for 3 h and left for 30 min to release bubbles formed during mixing. Then it was casted on a glass plate and dried in a hot air oven at 40°C for 24 h. The dried film of the charcoal-alginate membrane was immersed in a 3% $CaCl_2$ solution for 4 h for crosslinking. The fabricated membrane was washed three times with deionized water and dried in an oven at 50°C for 2 h. Dried membranes were kept in an airtight bottle until further use. The fabricated membrane is shown in Fig. S2.

2.3. Characterization

2.3.1. Instrumentations

Morphology of the fabricated membrane was analyzed by using scanning electron microscopy (SEM; Tescan VEGA XM variable pressure SEM, Brno-Czech Republic). The prepared membrane was analysed for Brunauer–Emmett–Teller (BET) surface area, pore-volume, and average pore size, using Nova Touch LX 2 surface area and pore size analyser (Quantachrome—Boynton Beach, FL, USA) with nitrogen purging at bath temperature 77.35 k.

FTIR analysis of the fabricated membrane before and after the reaction was performed by using Jasco FT/IR-6300 Instrument (Vector 22, Bruker, Massachusetts, MA, USA), IR scanning ranging from 400 to 4,000 cm^{-1}.

2.3.2. Water uptake

Water uptake of the fabricated membrane was determined by soaking accurately weighted dried membrane into distilled water at room temperature. After withdrawing the surface water with a tissue paper, the wet weight of the membrane was attained. Water uptake was calculated from the difference in mass before and after drying of the membrane by using Eq. (1) [41,42].

$$W_R = \frac{W_{WET} - W_{DRY}}{W_{DRY}} \times 100\% \quad (1)$$

where W_{WET} and W_{DRY} represent respectively the wet and dry weights of the prepared membrane.

2.4. RhB adsorption on the nanocomposite membrane

Adsorption of RhB from an aqueous solution onto nano-activated charcoal incorporated sodium alginate-based cross-linked membrane was performed using the procedure reported in our previous work [17,20,21,46–48] (Section S1 in supporting information for details).

2.5. Adsorption isotherms

Several adsorption isotherm models including Langmuir, Freundlich, Temkin and Dubinin–Radushkevich were utilized to investigate RhB adsorption onto the fabricated nano-activated charcoal incorporated sodium alginate-based cross-linked membrane (Section S2 in supporting information for details).

2.6. Adsorption kinetics

Kinetic models such as pseudo-first-order model, pseudo-second-order model, Elovich model, liquid-film diffusion model, modified Freundlich equation and Bangham equation were applied to study RhB adsorption from an aqueous solution onto the fabricated nano-activated charcoal incorporated sodium alginate-based cross-linked membrane (Section S3 in supporting information for details).

3. Results and discussion

3.1. Morphology and BET surface area

Morphology of the fabricated nano-activated charcoal incorporated sodium alginate-based cross-linked membrane was revealed in detail by using scanning electron microscopy (SEM). Fig. 1 depicts the SEM micrographs of blank alginate hydrogel membrane, surface and cross-section of the fabricated membrane. It was noted that the fabricated nano-activated charcoal incorporated sodium alginate-based cross-linked membrane exhibited rough structure. There were small cracks or hole on surface of the fabricated membrane. Therefore, it could serve as an efficient material for RhB adsorption from an aqueous solution.

The BET surface area of activated carbon membrane was calculated to be 82.721 m^2/g, from the $0.05 < P/P_0 > 0.35$ region of the adsorption curve. Isotherm plot represents type V hysteresis loop with capillary condensation, characteristic of mesoporous materials with irregular pore structure [1]. The average pore radius was 2.3056e + 02 nm indicating the mesoporous characteristics of membrane. The total pore volume measured was 9.5363e + 00 cc/g at a relative pressure of 0.97594 [49].

3.2. FTIR test

Fig. 2 represents IR spectra of the pristine sodium alginate membrane and fabricated cross-linked membrane. In the pristine membrane, the peaks observed at the region of 1,725 cm^{-1} are due to the carboxylic acid groups. The peaks observed at 1,034–1,036 cm^{-1} are corresponding to the C–O–C bonding [50]. The broad peaks at the wavelength ranging from 3,393 and 3,401 cm^{-1} were associated to –OH stretching vibration [50]. Moreover, two peaks which are noted at 1,601 and 1,390 cm^{-1} were due to the stretching vibration of asymmetric and symmetric COO– groups in the alginate [50,51]. The new bands at 2,400 and 2,800 cm^{-1} were seen into the fabricated nano-activated charcoal incorporated sodium alginate-based cross-linked membrane. It proved the successful fabrication of nano-activated charcoal incorporated sodium alginate-based cross-linked membrane.

FTIR was utilized to confirm RhB adsorption from an aqueous solution onto the fabricated membrane. Fig. 3 shows the FTIR spectrums of the fabricated nano-activated charcoal incorporated sodium alginate-based cross-linked membrane before and after RhB adsorption onto it. The changes in the intensities of the band were observed after RhB adsorption onto it. The changes in peak positions at 2,800; 2,600; 1,600 and 1,200 cm^{-1} were noted on RhB adsorption from an aqueous solution onto the fabricated membrane. Moreover, the peak intensities was also changed with it (Fig. 3). These changes in peak intensities proved the RhB adsorption on the fabricated membrane.

3.3. Water uptake

Water uptake is a crucial factor of the membrane. It showed the hydrophilicity of the fabricated membrane [20,45]. It has a significant effect on adsorption property of the fabricated membrane. For the fabricated membrane, the water uptake was found to be 43% at ambient temperature.

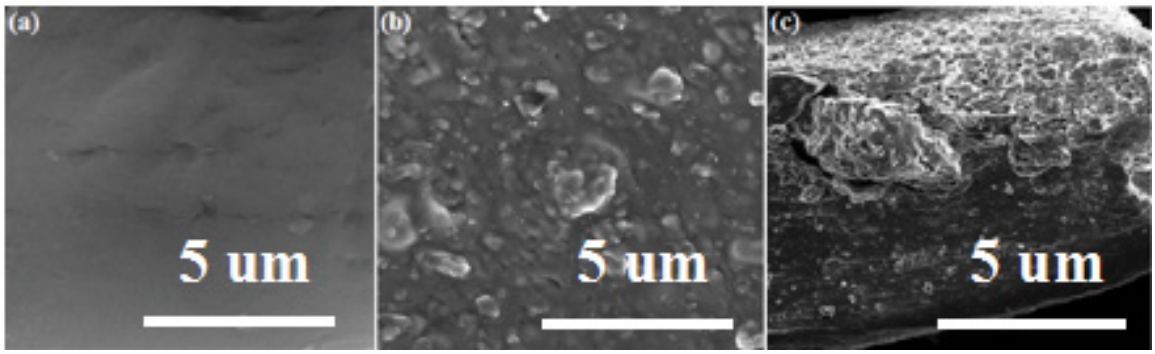

Fig. 1. (a) SEM micrographs of sodium alginate membrane, (b) surface of the fabricated nano-activated charcoal incorporated sodium alginate-based cross-linked membrane, and (c) cross-section of the fabricated nano-activated charcoal incorporated sodium alginate-based cross-linked membrane.

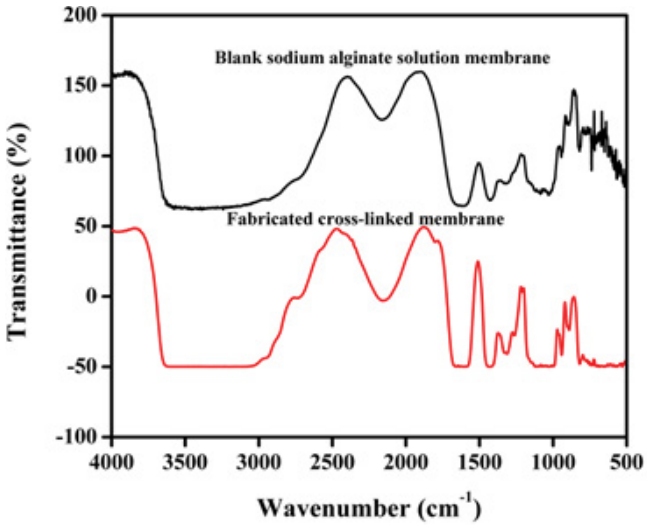

Fig. 2. FTIR spectrums of pristine sodium alginate membrane and fabricated cross-linked membrane.

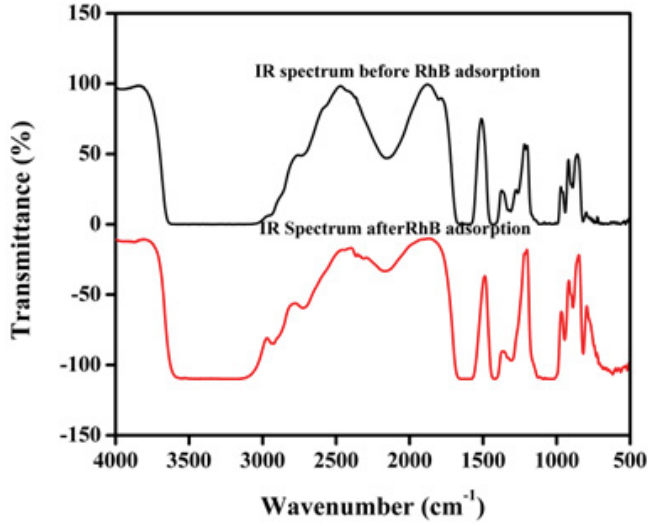

Fig. 3. IR spectrums of the nano-activated charcoal incorporated sodium alginate-based cross-linked membrane before and after RhB adsorption onto it.

From this, it was concluded that the nano-activated charcoal incorporated sodium alginate-based cross-linked membrane was convenient for RhB adsorption from an aqueous solution at room temperature.

3.4. Effect of operating factors on RhB removal from an aqueous solution

The effect of contact time on RhB removal from an aqueous solution by using nano-activated charcoal incorporated sodium alginate-based cross-linked membrane was investigated in detail. Fig. 4a represents the effect of contact time on the RhB removal from an aqueous solution at room temperature. Results showed that the percentage removal of RhB was increased with contact time. It was found to be increased from 17% to 97% with increasing contact time. Table 1 gives an interesting comparison of the RhB removal capability of the fabricated membrane with other adsorbent reported in literature. The equilibrium was attained after 2,880 min. The measured optimum time was employed to conduct further experiment. Result further indicates that the RhB percentage removal was rapid in initial stage and slowed down later. The fast RhB removal in first step was associated to the presence of several empty sites onto the fabricated membrane [20,52].

Fig. 4b shows the effect of mass of the fabricated nano-activated charcoal incorporated sodium alginate-based cross-linked membrane dosage on the percentage removal of RhB from an aqueous solution at room temperature. It was observed that the removal of RhB was enhanced from 50% to 98% with increase in dosage of the fabricated membrane from 0.10 to 0.30 g. It was associated to enhance in the number of available active sites with increasing the fabricated nano-activated charcoal hydrogel membrane from 0.10 to 0.30 g. The optimized dosage of the fabricated nano-activated charcoal incorporated sodium alginate-based cross-linked membrane (0.30 g) was used for further work because at this amount there was maximum RhB removal from an aqueous solution at room temperature. Our previous studied showed similar results [18,53].

The effect on initial concentration of RhB on the percentage removal of RhB from an aqueous solution by using the fabricated nano-activated charcoal incorporated sodium alginate-based cross-linked membrane was also studied. Fig. 4c represents the effect of initial concentration of RhB in an aqueous solution on the percentage RhB removal at room temperature. The percentage removal of RhB from an aqueous solution by using the fabricated nano-activated charcoal incorporated sodium alginate-based cross-linked membrane was declined with increasing initial concentration of RhB in an aqueous solution. The effect initial concentration of RhB on the percentage removal is shown in Fig. S3. Same results were attained in previous work [54–56]. Some of RhB was unabsorbed because of higher saturation of adsorption sites at higher initial concentration of RhB in an aqueous solution. At low concentration, more binding sites were present for adsorption of RhB. The number of RhB molecules competing for binding sites onto the fabricated nano-activated charcoal incorporated sodium alginate-based cross-linked membrane was enhanced with increasing concentration of dye.

3.5. Adsorption isotherms

Adsorption isotherms such as Langmuir, Freundlich, Temkin, Dubinin–Radushkevich were applied to investigate RhB adsorption from an aqueous solution onto the fabricated nano-activated charcoal incorporated sodium alginate-based cross-linked membrane. Fig. 5a represents the Langmuir isotherm for RhB adsorption onto the fabricated nano-activated charcoal incorporated sodium alginate-based cross-linked membrane. In this case, the correlation coefficient (R^2 = 0.877) value was close to unity. The determined value of parameters for it are given in Table 2. From this, we noted that RhB adsorption followed Langmuir adsorption isotherm. The R_L (0.13–0.74)

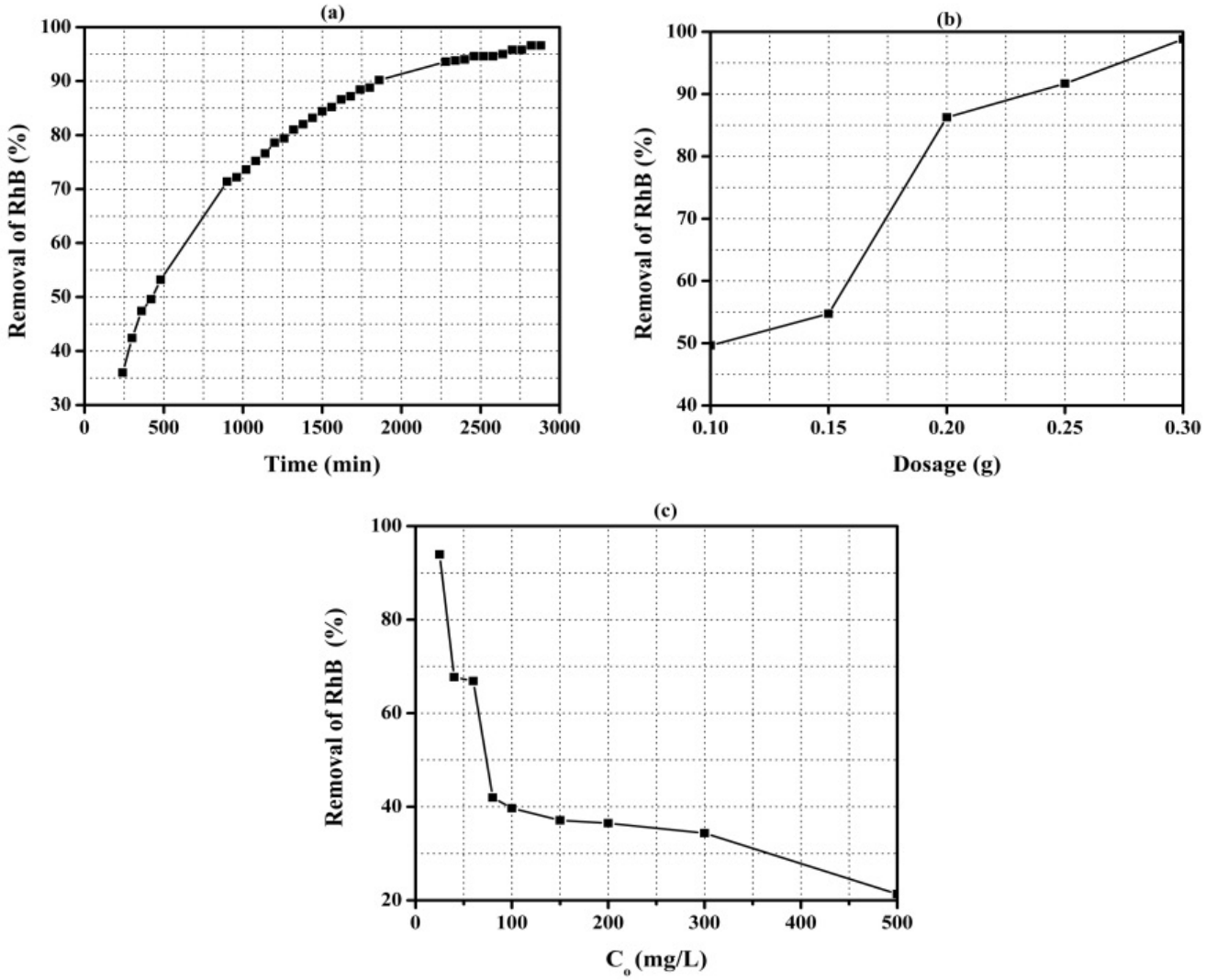

Fig. 4. (a) Effect of contact time, (b) effect of dosage, and (c) effect of initial concentration RhB on RhB removal from an aqueous solution by using the fabricated nano-activated charcoal incorporated sodium alginate-based cross-linked membrane.

Table 1
Comparison of adsorption performance of the fabricated membrane for RhB with other reported adsorbents

Adsorbent	Removal (%)	References
TRH	83.0	[21]
Fly ash based inorganic polymer	62.45	[1]
CMK-8 carbon replica	~100	[57]
Mesoporous silica (KIT-6)	65.0	[57]
Co-FeOOH/g-C_3N_4 composite	91.5	[58]
Activated biochar	54.0	[59]
P-CZIF-86	99.90	[60]
MgO-FCM-NP	99.0	[61]
A-rGO/cobalt oxide nanoparticles composite	95	[62]
Raphia hookeri fruit epicarp	89.0	[63]
Nano-activated charcoal incorporated sodium alginate-based cross-linked membrane	97.0	This work

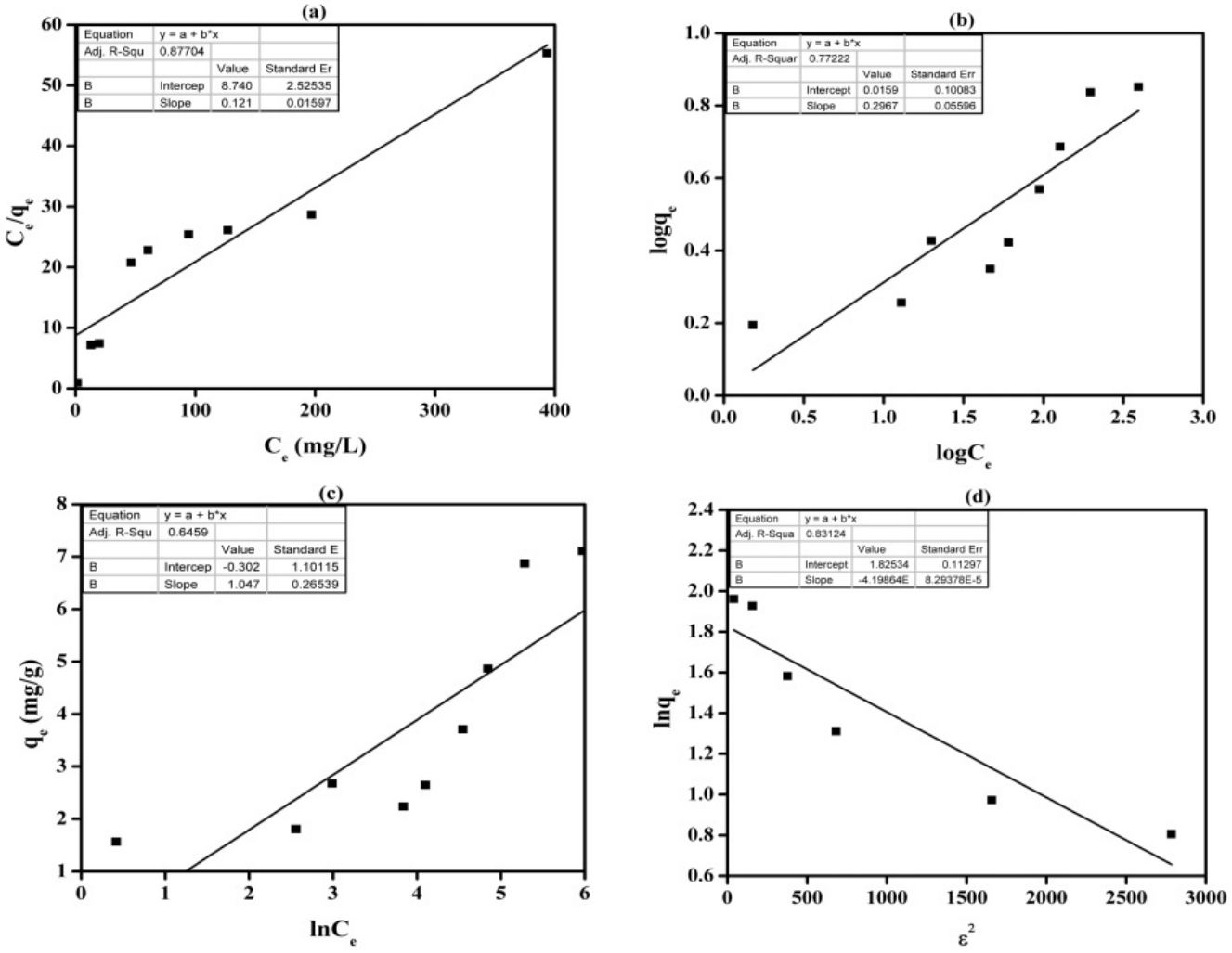

Fig. 5. (a) Langmuir isotherm, (b) Freundlich isotherm, (c) Temkin isotherm, (d) Dubinin–Radushkevich isotherm for RhB adsorption onto the fabricated nano-activated charcoal incorporated sodium alginate-based cross-linked membrane.

value showed that RhB adsorption was favorable process. Fig. 5b denotes Freundlich adsorption isotherm for RhB adsorption onto the fabricated nano-activated charcoal incorporated sodium alginate-based cross-linked membrane and the determined values of its factors (n and k_F) are given in Table 2. The correlation coefficient (R^2 = 0.772) value represented that RhB adsorption followed Freundlich adsorption isotherm. The determined value of Freundlich constant 'n' exhibited that RhB adsorption onto the fabricated nano-activated charcoal incorporated sodium alginate-based cross-linked membrane was good (Table 2). Temkin adsorption isotherm for RhB adsorption is depicted in Fig. 5c and the calculated values of b_T and A_T are shown Table 2. For Temkin isotherm, the correlation coefficient (R^2 = 0.646) value showed that RhB adsorption onto the fabricated nano-activated charcoal incorporated sodium alginate-based cross-linked membrane followed Temkin isotherm. Fig. 5d shows Dubinin–Radushkevich isotherm for adsorption of RhB onto the fabricated nano-activated charcoal incorporated sodium alginate-based cross-linked membrane. The calculated values of its factors are represented in Table 2. The measured mean adsorption energy was 34.50 kJ/mol. It showed that RhB adsorption was chemical adsorption process [56,64]. The value of E greater than 8 kJ/mol shows chemical ion exchange adsorption process whereas values of E below 8 kJ/mol were the characteristic of physical adsorption process [17].

3.6. Adsorption kinetics

Adsorption kinetics for RhB adsorption onto the fabricated nano-activated charcoal incorporated sodium alginate-based cross-linked membrane was explored by using several kinetic model including pseudo-first order model, pseudo-second-order model, Elovich model, liquid-film diffusion model, modified Freundlich equation and Bangham equation. The plot pseudo-first-order model for RhB adsorption is shown in Fig. 6a and the determined K_1 value is given in Table 3. There was a gap between experimental and calculated adsorption capacity (Table 3). The correlation

Table 2
Determined adsorption isotherms parameters for RhB adsorption onto the fabricated nano-activated charcoal incorporated sodium alginate-based cross-linked membrane

Adsorption isotherms	Determined parameters	
Langmuir isotherm	Q_m	8.21
	$K_L \times 10^{-2}$	1.40
	R_L	0.13–0.74
	R^2	0.877
Freundlich isotherm	n	3.37
	k_F	1.04
	R^2	0.772
Temkin isotherm	b_T	2365
	A_T	0.750
	R^2	0.646
Dubinin–Radushkevich isotherm	$\beta \times 10^{-4}$	4.20
	Q_m	6.20
	E	34.50
	R^2	0.831

Q_m (mg/g); K_L (L/mol); k_F ((mg/g)(L/mg)$^{1/n}$); C_m (mol/g); β (mol^2/J^2); E (kJ/mol).

coefficient (R^2 = 0.908) value was less than unity. From this, it was concluded that it does not explain the rate process.

Fig. 6b depicts pseudo-second-order model for RhB adsorption onto the fabricated nano-activated charcoal incorporated sodium alginate-based cross-linked membrane and the determined adsorption capacity (q_e) value is given in Table 3. Here, the correlation coefficient (R^2 = 0.999) value was close to unity. This calculated adsorption capacity (1.92 mg/g) value was in good agreement with the experimental value (1.61 mg/g). It represented that RhB adsorption followed pseudo-second-order model.

The plot Elovich model is represented in Fig. 6c and its calculated values of the factors (α and β) are represented in Table 3. The correlation coefficient (R^2 = 0.993) value was smaller than pseudo-second-order model. Hence it is not good to explain RhB adsorption from an aqueous solution onto the fabricated nano-activated charcoal incorporated sodium alginate-based cross-linked membrane.

Fig. 6d shows the plot of liquid-film diffusion model and the measured value of K_{fd} is represented in Table 3. For it, the correlation coefficient (R^2 = 0.971) value was lower than pseudo-second-order model. Therefore, this model is not sufficient to explain RhB adsorption onto the fabricated nano-activated charcoal incorporated sodium alginate-based cross-linked membrane.

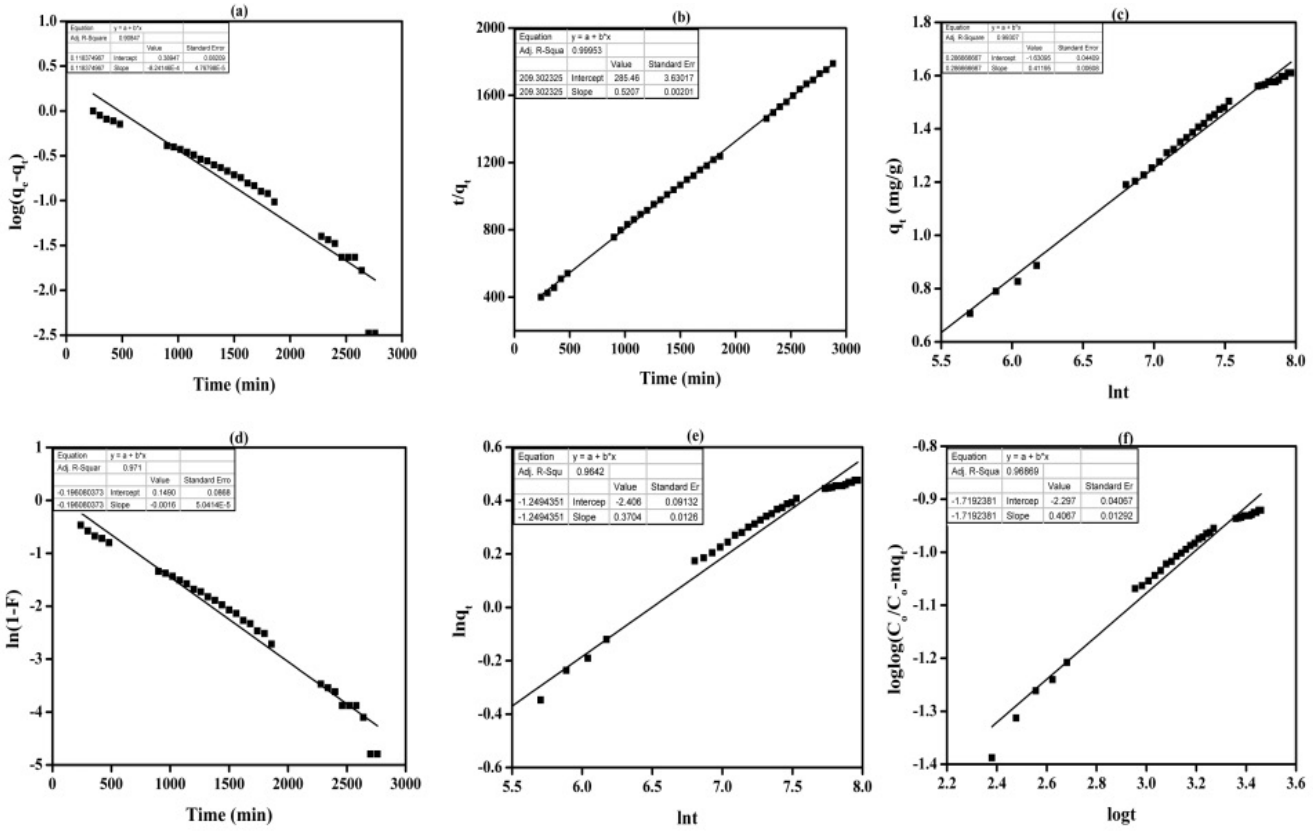

Fig. 6. (a) Pseudo-first-order model, (b) pseudo-second-order model, (c) Elovich model, (d) liquid-film diffusion model, (e) modified Freundlich equation, (f) Bangham equation for RhB adsorption onto the fabricated nano-activated charcoal incorporated sodium alginate-based cross-linked membrane.

Table 3
Determined kinetics parameters for RhB adsorption onto the fabricated nano-activated charcoal incorporated sodium alginate-based cross-linked membrane

Adsorption kinetic models	Determined parameters	
Pseudo-first-order model	$q_{e,\text{exp.}}$	1.61
	q_e	2.45
	$K_1 \times 10^{-4}$	8.24
	R^2	0.908
Pseudo-first-order model	q_e	1.92
	$K_2 \times 10^{-4}$	9.52
	R^2	0.999
Elovich model	A	0.01
	B	2.43
	R^2	0.993
Liquid-film diffusion model	$K_{\text{fd}} \times 10^{-3}$	1.60
	C_{fd}	0.15
	R^2	0.971
Modified Freundlich equation	M	2.70
	$k \times 10^{-3}$	3.59
	R^2	0.964
Bangham equation	A	0.41
	$k_o \times 10^{-4}$	7.50
	R^2	0.968

q_e (mg/g); K_1: (min^{-1}); K_2 (g/mg·min); α (mg/g·min); β (g/mg); K_{fd}: (min^{-1}); k (L/g·min); k_o (mL/g·L).

The modified Freundlich equation's plot is depicted in Fig. 6e. The measured values of factors (m and k) for it are given in Table 3. The correlation coefficient (R^2 = 0.964) value for it was less than pseudo-second-order model. It showed that modified Freundlich equation not convenient to discuss RhB's adsorption.

Bangham equation's plot for RhB adsorption is depicted in Fig. 6f and the determined values of its factors (α and m) are shown in Table 3. The double logarithmic plot did not give linear curves depicting that the diffusion of RhB into pores of the fabricated nano-activated charcoal incorporated sodium alginate-based cross-linked membrane is not the only rate controlling step [65,66]. It may be that both film and pore diffusion were significant to different extent for RhB adsorption from an aqueous solution.

4. Conclusions

In summery the nano-activated charcoal incorporated sodium alginate-based cross-linked membrane was fabricated successfully by solution casting method. The fabricated membrane represented rough morphology. It exhibited water uptake of 43%. The fabrication of membrane was confirmed by FTIR spectroscopy. The removal of RhB was increased with contact time and membrane dosage while decreased with initial concentration of RhB in an aqueous solution. Adsorption isotherm demonstration represented that experimental data for RhB adsorption best fitted to Langmuir isotherm. Moreover, adsorption isotherm investigation showed that adsorption of RhB onto the nano-activated charcoal incorporated sodium alginate-based cross-linked membrane was chemical adsorption process with mean adsorption energy 34.50 kJ/mol. Kinetic studies showed that RhB adsorption fitted to pseudo-second-order model. From these results, it was concluded that the fabricated membrane is efficient for RhB removal from an aqueous solution at room temperature presenting a maximum removal of 98%.

Acknowledgements

The authors are highly thankful to University of Sharjah (UOS), Sharjah, United Arab Emirates for financial supports.

References

[1] M. El Alouani, S. Alehyen, H. El Hadki, H. Saufi, A. Elhalil, O.K. Kabbaj, M. Taibi, Synergetic influence between adsorption and photodegradation of Rhodamine B using synthesized fly ash based inorganic polymer, Surf. Interfaces, 24 (2021) 101136, doi: 10.1016/j.surfin.2021.101136.
[2] H. Ait Ahsaine, M. Zbair, Z. Anfar, Y. Naciri, R. El haouti, N. El Alem, M. Ezahri, Cationic dyes adsorption onto high surface area 'almond shell' activated carbon: kinetics, equilibrium isotherms and surface statistical modeling, Mater. Today Chem., 8 (2018) 121–132.
[3] M. Sundararajan, V. Sailaja, L. John Kennedy, J. Judith Vijaya, Photocatalytic degradation of rhodamine B under visible light using nanostructured zinc doped cobalt ferrite: kinetics and mechanism, Ceram. Int., 43 (2017) 540–548.
[4] P.C. Vandevivere, R. Bianchi, W. Verstraete, Review: treatment and reuse of wastewater from the textile wet-processing industry: review of emerging technologies, J. Chem. Technol. Biotechnol., 72 (1998) 289–302.
[5] Y.M. Slokar, A.M. Le Marechal, Methods of decoloration of textile wastewaters, Dyes Pigm., 37 (1998) 335–356.
[6] M.I. Khan, S. Zafar, M.A. Khan, F. Mumtaz, P. Prapamonthon, A.R. Buzdar, Bougainvillea glabra leaves for adsorption of congo red from wastewater, Fresenius Environ. Bull., 27 (2018) 1456–1465.
[7] S. Wang, Z. Zhu, A. Coomes, F. Haghseresht, G. Lu, The physical and surface chemical characteristics of activated carbons and the adsorption of methylene blue from wastewater, J. Colloid Interface Sci., 284 (2005) 440–446.
[8] M.I. Khan, S. Zafar, A.R. Buzdar, M.F. Azhar, W. Hassan, A. Aziz, Use of citrus sinensis leaves as a bioadsorbent for removal of congo red dye from aqueous solution, Fresenius Environ. Bull., 27 (2018) 4679–4688.
[9] S. Soni, P.K. Bajpai, J. Mittal, C. Arora, Utilisation of cobalt doped iron based MOF for enhanced removal and recovery of methylene blue dye from waste water, J. Mol. Liq., 314 (2020) 113642, doi: 10.1016/j.molliq.2020.113642.
[10] S.S. Asha Patel, J. Mittal, A. Mittal, C. Arora, Sequestration of crystal violet from aqueous solution using ash of black turmeric rhizome, Desal. Water Treat., 220 (2021) 342–352.
[11] P.K. Charu Arora, S. Soni, J. Mittal, A. Mittal, B. Singh, Efficient removal of malachite green dye from aqueous solution using *Curcuma caesia* based activated carbon, Desal. Water Treat., 195 (2020) 341–352.
[12] C. Arora, S. Soni, S. Sahu, J. Mittal, P. Kumar, P.K. Bajpai, Iron based metal organic framework for efficient removal of methylene blue dye from industrial waste, J. Mol. Liq., 284 (2019) 343–352.
[13] M. Ahmed, R. Ram, Removal of basic dye from waste-water using silica as adsorbent, Environ. Pollut., 77 (1992) 79–86.
[14] A. Mariyam, J. Mittal, F. Sakina, R.T. Baker, A.K. Sharma, A. Mittal, Efficient batch and fixed-bed sequestration of a basic dye using a novel variant of ordered mesoporous carbon as adsorbent, Arabian J. Chem., 14 (2021) 103186, doi: 10.1016/j.arabjc.2021.103186.

[15] A. Çelekli, S.S. Birecikligil, F. Geyik, H. Bozkurt, Prediction of removal efficiency of Lanaset Red G on walnut husk using artificial neural network model, Bioresour. Technol., 103 (2012) 64–70.
[16] H. Zhu, R. Jiang, Y.-Q. Fu, J.-H. Jiang, L. Xiao, G.-M. Zeng, Preparation, characterization and dye adsorption properties of γ-Fe_2O_3/SiO_2/chitosan composite, Appl. Surf. Sci., 258 (2011) 1337–1344.
[17] M.I. Khana, A. Shanableh, N. Nasir, S. Shahida, Adsorptive removal of methyl orange from wastewaters by the commercial anion exchange membrane EPTAC, Desal. Water Treat., 234 (2021) 245–254.
[18] M.I. Khan, M.H. Lashari, M. Khraisheh, S. Shahida, S. Zafar, P. Prapamonthon, A. Rehman, S. Anjum, N. Akhtar, F. Hanif, Adsorption kinetic, equilibrium and thermodynamic studies of Eosin-B onto anion exchange membrane, Desal. Water Treat., 155 (2019) 84–93.
[19] M.I. Khan, J. Su, L. Guo, Development of triethanolamine functionalized-anion exchange membrane for adsorptive removal of methyl orange from aqueous solution, Desal. Water Treat., 209 (2021) 342–352.
[20] M.I. Khan, A. Shanableh, J. Fernandez, M.H. Lashari, S. Shahida, S. Manzoor, S. Zafar, A. ur Rehman, N. Elboughdiri, Synthesis of DMEA-grafted anion exchange membrane for adsorptive discharge of methyl orange from wastewaters, Membranes, 11 (2021) 166, doi: 10.3390/membranes11030166.
[21] M.I. Khan, A. Shanableh, Adsorption of Rhodamine B from an aqueous solution onto NaOH-treated rice husk, Desal. Water Treat., 252 (2022) 104–115.
[22] M.I. Khan, S. Zafar, M.F. Azhar, A.R. Buzdar, W. Hassan, A. Aziz, M. Khraisheh, Leaves powder of syzgium cumini as an adsorbent for removal of congo red dye from aqueous solution, Fresenius Environ. Bull., 27 (2018) 3342–3350.
[23] R.-k. Xu, S.-c. Xiao, J.-h. Yuan, A.-z. Zhao, Adsorption of methyl violet from aqueous solutions by the biochars derived from crop residues, Bioresour. Technol., 102 (2011) 10293–10298.
[24] T. Farías, L.C. de Ménorval, J. Zajac, A. Rivera, Benzalkonium chloride and sulfamethoxazole adsorption onto natural clinoptilolite: effect of time, ionic strength, pH and temperature, J. Colloid Interface Sci., 363 (2011) 465–475.
[25] Y. Feng, F. Yang, Y. Wang, L. Ma, Y. Wu, P.G. Kerr, L. Yang, Basic dye adsorption onto an agro-based waste material–Sesame hull (*Sesamum indicum* L.), Bioresour. Technol., 102 (2011) 10280–10285.
[26] Y. Yang, D. Jin, G. Wang, D. Liu, X. Jia, Y. Zhao, Biosorption of Acid Blue 25 by unmodified and CPC-modified biomass of Penicillium YW01: kinetic study, equilibrium isotherm and FTIR analysis, Colloids Surf., B, 88 (2011) 521–526.
[27] M. Akgül, A. Karabakan, Promoted dye adsorption performance over desilicated natural zeolite, Microporous Mesoporous Mater., 145 (2011) 157–164.
[28] X.-Y. Huang, H.-T. Bu, G.-B. Jiang, M.-H. Zeng, Cross-linked succinyl chitosan as an adsorbent for the removal of Methylene Blue from aqueous solution, Int. J. Biol. Macromol., 49 (2011) 643–651.
[29] T. Kan, X. Jiang, L. Zhou, M. Yang, M. Duan, P. Liu, X. Jiang, Removal of methyl orange from aqueous solutions using a bentonite modified with a new gemini surfactant, Appl. Clay Sci., 54 (2011) 184–187.
[30] B. Balci, Basic textile dye adsorption from aqueous solution and synthetic dye bath wastewater by modified eucalyptus barks, Fresenius Environ. Bull., 25 (2016) 6124–6131.
[31] A. Xue, S. Zhou, Y. Zhao, X. Lu, P. Han, Effective NH_2-grafting on attapulgite surfaces for adsorption of reactive dyes, J. Hazard. Mater., 194 (2011) 7–14.
[32] K. Elass, A. Laachach, A. Alaoui, M. Azzi, Removal of methyl violet from aqueous solution using a stevensite-rich clay from Morocco, Appl. Clay Sci., 54 (2011) 90–96.
[33] G. Lv, Z. Li, W.-T. Jiang, P.-H. Chang, J.-S. Jean, K.-H. Lin, Mechanism of acridine orange removal from water by low-charge swelling clays, Chem. Eng. J., 174 (2011) 603–611.
[34] H. Chen, J. Zhao, A. Zhong, Y. Jin, Removal capacity and adsorption mechanism of heat-treated palygorskite clay for methylene blue, Chem. Eng. J., 174 (2011) 143–150.
[35] M. Ghaedi, H. Hossainian, M. Montazerozohori, A. Shokrollahi, F. Shojaipour, M. Soylak, M. Purkait, A novel acorn based adsorbent for the removal of brilliant green, Desalination, 281 (2011) 226–233.
[36] A.Y. Dursun, O. Tepe, Removal of Chemazol Reactive Red 195 from aqueous solution by dehydrated beet pulp carbon, J. Hazard. Mater., 194 (2011) 303–311.
[37] J.d.J. da Silveira Neta, G.C. Moreira, C.J. da Silva, C. Reis, E.L. Reis, Use of polyurethane foams for the removal of the Direct Red 80 and Reactive Blue 21 dyes in aqueous medium, Desalination, 281 (2011) 55–60.
[38] C. Arora, S. Sonia, P. Bajpaib, J. Mittalc, A. Mariyam, Dye Removal from Wastewater using Metal–Organic Frameworks, Management of Contaminants of Emerging Concern (CEC) in Environment, 2021.
[39] Y. Diquarternasi, Removal of basic blue 3 and reactive orange 16 by adsorption onto quartenized sugar cane bagasse, Malaysian J. Anal. Sci., 13 (2009) 185–193.
[40] P.K.B. Sanju Sonia, D. Bharti, J. Mittal, C. Arora, Removal of crystal violet from aqueous solution using iron based metal organic framework, Desal. Water Treat., 205 (2020) 386–399.
[41] M.I. Khan, C. Zheng, A.N. Mondal, M.M. Hossain, B. Wu, K. Emmanuel, L. Wu, T. Xu, Preparation of anion exchange membranes from BPPO and dimethylethanolamine for electrodialysis, Desalination, 402 (2017) 10–18.
[42] M.I. Khan, A.N. Mondal, B. Tong, C. Jiang, K. Emmanuel, Z. Yang, L. Wu, T. Xu, Development of BPPO-based anion exchange membranes for electrodialysis desalination applications, Desalination, 391 (2016) 61–68.
[43] M.I. Khan, M. Khraisheh, F. Almomani, Fabrication and characterization of pyridinium functionalized anion exchange membranes for acid recovery, Sci. Total Environ., 686 (2019) 90–96.
[44] M.I. Khan, X. Li, J. Fernandez-Garcia, M.H. Lashari, A. ur Rehman, N. Elboughdiri, L. Kolsi, D. Ghernaout, Effect of different quaternary ammonium groups on the hydroxide conductivity and stability of anion exchange membranes, ACS Omega, 6 (2021) 7994–8001.
[45] M.I. Khan, J. Fernandez-Garcia, Q.-L. Zhu, Fabrication of doubly charged anion-exchange membranes for enhancing hydroxide conductivity, Sep. Sci. Technol., 56 (2020) 1589–1600.
[46] M.I. Khan, L. Wu, A.N. Mondal, Z. Yao, L. Ge, T. Xu, Adsorption of methyl orange from aqueous solution on anion exchange membranes: adsorption kinetics and equilibrium, Membr. Water Treat., 7 (2016) 23–38.
[47] M.I. Khan, M.A. Khan, S. Zafar, S.A. Hussain, Adsorption kinetics and thermodynamics ttudy for the removal of anionic dye Eosin-B From aqueous solution by anion exchange membrane: adsorption kinetics and themodynamics, Sch. J. Eng. Technol., 3 (2015) 741–749.
[48] M.I. Khan, A. Shanableh, N. Elboughdiri, M.H. Lashari, S. Manzoor, S. Shahida, N. Farooq, Y. Bouazzi, S. Rejeb, Z. Elleuch, K. Kriaa, A. ur Rehman, Adsorption of methyl orange from an aqueous solution onto a BPPO-based anion exchange membrane, ACS Omega, 7 (2022) 26788–26799.
[49] K.V. Kumar, S. Gadipelli, B. Wood, K.A. Ramisetty, A.A. Stewart, C.A. Howard, D.J.L. Brett, F. Rodriguez-Reinoso, Characterization of the adsorption site energies and heterogeneous surfaces of porous materials, J. Mater. Chem. A, 7 (2019) 10104–10137.
[50] F. Ugur Nigiz, Graphene oxide-sodium alginate membrane for seawater desalination through pervaporation, Desalination, 485 (2020) 114465, doi: 10.1016/j.desal.2020.114465.
[51] H. Zheng, J. Yang, S. Han, The synthesis and characteristics of sodium alginate/graphene oxide composite films crosslinked with multivalent cations, J. Appl. Polym. Sci., 133 (2016), doi: 10.1002/app.43616.
[52] M.I. Khan, A. Shanableh, N. Elboughdiri, M.H. Lashari, S. Shahida, Application of the commercial anion exchange membrane for adsorptive removal of Eriochrome Black-T from aqueous solution, Desal. Water Treat., 252 (2022) 437–448.
[53] M.I. Khan, T.M. Ansari, S. Zafar, A.R. Buzdar, M.A. Khan, F. Mumtaz, P. Prapamonthon, M. Akhtar, Acid green-25

removal from wastewater by anion exchange membrane: adsorption kinetic and thermodynamic studies, Membr. Water Treat., 9 (2018) 79–85.
[54] S. Zafar, M.I. Khan, A. Shanableh, S. Ahmad, S. Manzoor, S. Shahida, P. Prapamonthon, S. Mubeen, A. Rehman, Adsorption of silver, thorium and nickel ions from aqueous solution onto rice husk, Desal. Water Treat., 236 (2021) 108–122.
[55] S. Zafar, M.I. Khan, W. Hassan, S. Mubeen,T. Javed, S. Shahida, S. Manzoor, A. Shanableh, A. Rehman, M.L. Mirza, N. Khalid, M.H. Lashari, Application of NaOH-treated rice husk for adsorptive discharge of cobalt ions from wastewater, Desal. Water Treat., 226 (2021) 328–338.
[56] S. Zafar, M.I. Khan, H. Rehman, J. Fernandez-Garcia, S. Shahida, P. Prapamonthon, M. Khraisheh, A. Rehman, H.B. Ahmad, M.L. Mirza, N. Khalid, M.H. Lashari, Kinetic, equilibrium, and thermodynamic studies for adsorptive removal of cobalt ions by rice husk from aqueous solution, Desal. Water Treat., 204 (2020) 285–296.
[57] J.B. Goes e Silva, E. Rigoti, S. Pergher, Rhodamine B adsorption in ordered mesoporous materials: a comparison efficiency on KIT-6 and CMK-8, Results Mater., 9 (2021) 100162, doi: 10.1016/j.rinma.2020.100162.
[58] W.D.S. Siyang, Z. Huanxin, C. Yu, W. Xin, Z. Yu, Fabrication of Co-FeOOH/g-C_3N_4 composite and its catalytic performance on heterogeneous photo-Fenton, Chin. J. Environ. Eng., 14 (2020) 3262–3269.
[59] F.A. Adekola, S.B. Ayodele, A.A. Inyinbor, Activated biochar prepared from plaintain peels: characterization and Rhodamine B adsorption data set, Chem. Data Collect., 19 (2019) 100170, doi: 10.1016/j.cdc.2018.11.012.
[60] J. Zhang, X. Hu, X. Yan, R. Feng, M. Zhou, J. Xue, Enhanced adsorption of Rhodamine B by magnetic nitrogen-doped porous carbon prepared from bimetallic ZIFs, Colloids Surf., A, 575 (2019) 10–17.
[61] S. Rahdar, A. Rahdar, M.N. Zafar, S.S. Shafqat, S. Ahmadi, Synthesis and characterization of MgO supported Fe–Co–Mn nanoparticles with exceptionally high adsorption capacity for Rhodamine B dye, J. Mater. Res. Technol., 8 (2019) 3800–3810.
[62] S.H. Alwan, H.A.H. Alshamsi, L.S. Jasim, Rhodamine B removal on A-rGO/cobalt oxide nanoparticles composite by adsorption from contaminated water, J. Mol. Struct., 1161 (2018) 356–365.
[63] A.A. Inyinbor, F.A. Adekola, G.A. Olatunji, Kinetics, isotherms and thermodynamic modeling of liquid phase adsorption of Rhodamine B dye onto *Raphia hookeri* fruit epicarp, Water Resour. Ind., 15 (2016) 14–27.
[64] S. Zafar, M.I. Khan, M.H. Lashari, M. Khraisheh, F. Almomani, M.L. Mirza, N. Khalid, Removal of copper ions from aqueous solution using NaOH-treated rice husk, Emerg. Mater., 3 (2020) 857–870.
[65] M.I. Khan, S. Akhtar, S. Zafar, A. Shaheen, M.A. Khan, R. Luque, Removal of Congo red from aqueous solution by anion exchange membrane (EBTAC): adsorption kinetics and themodynamics, Materials, 8 (2015) 4147–4161.
[66] M.A. Khan, M.I. Khan, S. Zafar, Removal of different anionic dyes from aqueous solution by anion exchange membrane, Membr. Water Treat., 8 (2016) 259–277.

Supporting information

S1. RhB adsorption on the nanocomposite membrane

Firstly, an aqueous solution of RhB was prepared into distilled water. To find out the optimized contact time, 3.75 g of the nano-activated charcoal incorporated sodium alginate-based cross-linked membrane was shaked into 250 mL of RhB aqueous solution with initial concentration of RhB 25 mg/L into an aqueous solution at room temperature with varying time intervals ranging from 0 to 2,880 min at shaking speed of 200 rpm. The optimized dosage of the fabricated membrane was determined by shaking its varying mass from 0.10 to 0.40 g into measured volume of RhB aqueous solution (250 mL) for specific time (2,880 min) at room temperature with initial concentration of RhB into an aqueous solution 25 mg/L at shaking speed of 200 rpm. To investigate adsorption isotherm, the measured mass of the prepared membrane was shaked into 250 mL of an aqueous solution with different concentration of RhB ranging from 25 to 500 mg/L at room temperature for 2,880 min at shaking speed of 200 rpm. The concentration of RhB was determined by using UV-VIS Spectrophotometer (UV-2550, Shimadzu, Kyoto, Japan) by finding the absorbance of the supernatant at wavelength (λ_{max} = 554 nm for RhB). The RhB concentration was calculated from the calibration curve. The RhB adsorbed onto the fabricated membrane at time *t*, was determined by using Eq. (S1):

$$q_t = \frac{C_0 - C_t}{W} \times V \tag{S1}$$

where C_o and C_t denote the RhB concentration at initial state and at time *t*, respectively. Similarly *V* and *W* are volume of RhB aqueous solution and weight of the membrane, respectively.

S2. Adsorption isotherms

S2.1. Langmuir isotherm

Langmuir isotherm is based on the maximum adsorption corresponds to the saturated monolayer of liquid molecules on the solid surface. It is represented as [S1]:

$$\frac{C_e}{q_e} = \frac{1}{K_L Q_m} + \frac{C_e}{Q_m} \tag{S2}$$

where K_L is Langmuir constant (L/mg), C_e is supernatant concentration at equilibrium state of the system (mg/L)and Q_m is Langmuir monolayers adsorption capacity (mg/g), and q_e is the amount of dye adsorbed at equilibrium state of system (mg/g). Its significant characteristics can be given in term of dimensionless constant separation factor R_L that is express by [S2]:

$$R_L = \frac{1}{1 + K_L C_0} \tag{S3}$$

The value of R_L denoted the shape of the isotherm to be either unfavorable (R_L > 1), linear (R_L = 1), favorable (0 < R_L > 0), or irreversible (R_L = 0) [S3].

S2.2. Freundlich isotherm

Freundlich isotherm is an empirical equation employed to discuss the heterogeneous system. It is shown as [S4]:

$$\log q_e = K_f + \frac{1}{n} \log C_e \tag{S4}$$

where K_f and n_F are Freundlich constant.

S2.3. Temkin isotherm

Temkin isotherm is denoted as [S5]:

$$q_e = B_T \ln A_T + B_T \ln C_e \tag{S5}$$

where $B_T = RT/b_T$, R is gas constant (8.31 J/mol K) and T is absolute temperature (K). The constant b_T is related to the heat of adsorption and A_T is equilibrium binding constant coinciding to the maximum binding energy.

S2.4. Dubinin–Radushkevich isotherm

Dubinin–Radushkevich isotherm is shown as [S5]:

$$\ln q_e = \ln q_m - \beta\varepsilon^2 \tag{S6}$$

where β (mol²/KJ) is constant related to the adsorption energy and ε is the Polanyi potential can be determined by using Eq. (S7):

$$\varepsilon = RT \ln\left(1 + \frac{1}{C_e}\right) \tag{S7}$$

where R is gas constant (8.31 kJ/mol) and T is absolute temperature (K). The mean free energy E (kJ/mol) can be measured by using Eq. (S8):

$$E = \frac{1}{\sqrt{2\beta}} \tag{S8}$$

S3. Adsorption kinetics

S3.1. Pseudo-first-order model

Lagergren pseudo-first-order rate is shown as [S6–S9]:

$$\log\left(q_e - q_t\right) = \log q_e - \frac{K_1 t}{2.303} \tag{S9}$$

where K_1 (min⁻¹), q_e (mg/g) and q_t (mg/g) denote rate constant of pseudo-first-order model, concentration of RhB adsorbed at equilibrium and time t respectively.

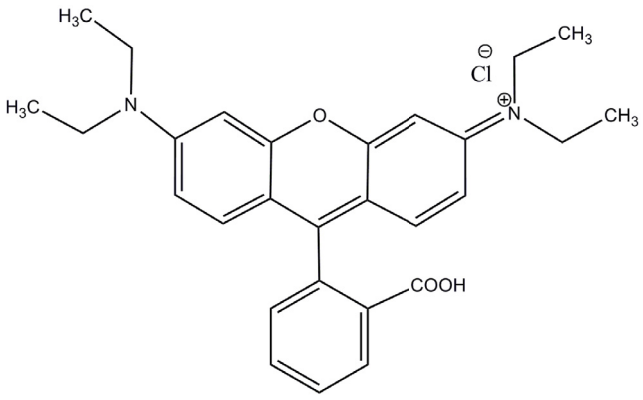

Fig. S1. Chemical structure of Rhodamine B dye.

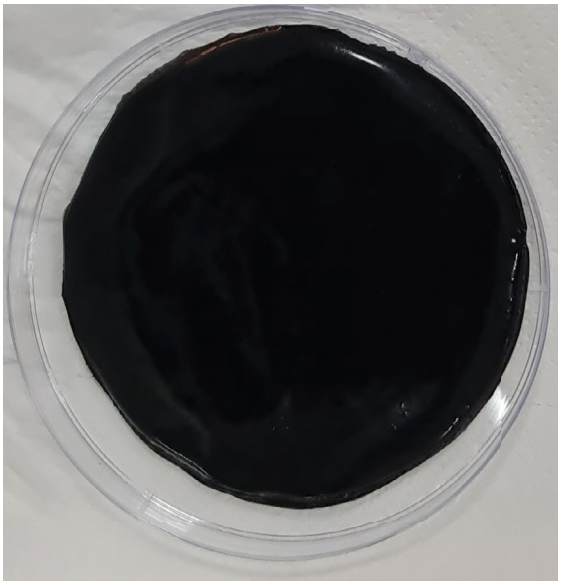

Fig. S2. Image of the fabricated nano-activated charcoal incorporated sodium alginate-based cross-linked membrane.

Fig. S3. (a) RhB aqueous solution before adsorption and (b) RhB aqueous solution after adsorption onto the fabricated nano-activated charcoal incorporated sodium alginate-based cross-linked membrane.

S3.2. Pseudo-second-order model

Pseudo-second-order kinetic model is represented as [S9–S11]:

$$\frac{t}{q_t} = \frac{1}{k_2 q_e^2} + \frac{t}{q_e} \tag{S10}$$

where K_2 (g/mg·min) is the rate constant of pseudo-second-order model.

S3.3. Elovich model

Elovich model is expressed as [S12,S13]:

$$q_t = \frac{1}{\beta}\ln\left(\alpha\beta\right) + \frac{1}{\beta}\ln t \tag{S11}$$

where α (mg/g min) and β (g/mg) are constant. The parameter α is initial adsorption rate and β is the extent of surface coverage and activation energy for chemisorption.

S3.4. Liquid-film diffusion model

It is denoted as [S14]:

$$\ln\left(1-F\right) = -K_{\text{fd}}t \tag{S12}$$

where K_{fd} is liquid-film diffusion rate constant and $F = q_t/q$.

S3.5. Modified Freundlich equation

It was developed by Kuo and Lotse [S10,S15]:

$$q_t = kC_0 t^{1/m} \tag{S13}$$

where C_o, k, t and m are initial concentration (mg/L), adsorption rate constant (L/g·min), contact time (min^{-1}) and the Kuo–Lotse constant respectively. Its linear form is represented as:

$$\ln q_t = \ln\left(kC_0\right) + \frac{1}{m}\ln t \tag{S14}$$

S3.6. Bangham equation

Bangham equation is shown as [S9,S13]:

$$\log\log\left(\frac{C_0}{C_0 - q_1 m}\right) = \log\left(\frac{k_0 m}{2.303V}\right) + \alpha\log t \tag{15}$$

where m is mass of the fabricated (adsorbent) used (g/L), V is volume of RhB dye solution (mL), α (<1) and k_o (mL/(g/L)) are constants.

References

[S1] I. Langmuir, The constitution and fundamental properties of solids and liquids, J. Franklin Inst., 183 (1917) 102–105.

[S2] T.W. Weber, R.K. Chakravorti, Pore and solid diffusion models for fixed-bed adsorbers, AlChE J., 20 (1974) 228–238.

[S3] G. McKay, Adsorption of dyestuffs from aqueous solutions with activated carbon I: equilibrium and batch contact-time studies, J. Chem. Technol. Biotechnol., 32 (1982) 759–772.

[S4] H. Freundlich, Uber die adsorption in lasugen (Leipzig), Z. Phys. Chem. A, 57 (1906) 385–470.

[S5] M..I. Khan, S. Zafar, M.A. Khan, F. Mumtaz, P. Prapamonthon, A.R. Buzdar, Bougainvillea glabra leaves for adsorption of congo red from wastewater, Fresenius Environ. Bull., 27 (2018) 1456–1465.

[S6] S. Zafar, M.I. Khan, M. Khraisheh, S. Shahida,T. Javed, M.L. Mirza, N. Khalid, Use of rice husk as an efective sorbent for the removal of cerium ions from aqueous solution: kinetic, equilibrium and thermodynamic studies, Desal. Water Treat., 150 (2019) 124–135.

[S7] M.I. Khan, S. Zafar, A.R. Buzdar, M.F. Azhar, W. Hassan, A. Aziz, Use of citrus sinensis leaves as a bioadsorbent for removal of congo red dye from aqueous solution, Fresenius Environ. Bull., 27 (2018) 4679–4688.

[S8] M.I. Khan, S. Zafar, M.F. Azhar, A.R. Buzdar, W. Hassan, A. Aziz, M. Khraisheh, Leaves powder of syzgium cumini as an adsorbent for removal of congo red dye from aqueous solution, Fresenius Environ. Bull., 27 (2018) 3342–3350.

[S9] M.I. Khan, A. Shanableh, J. Fernandez, M.H. Lashari, S. Shahida, S. Manzoor, S. Zafar, A. ur Rehman, N. Elboughdiri, Synthesis of DMEA-grafted anion exchange membrane for adsorptive discharge of methyl orange from wastewaters, Membranes, 11 (2021) 166, doi: 10.3390/membranes11030166.

[S10] M.I. Khan, M.H. Lashari, M. Khraisheh, S. Shahida, S. Zafar, P. Prapamonthon, A. Rehman, S. Anjum, N. Akhtar, F. Hanif, Adsorption kinetic, equilibrium and thermodynamic studies of Eosin-B onto anion exchange membrane, Desal. Water Treat., 155 (2019) 84–93.

[S11] I.W. Almanassra, V. Kochkodan, G. McKay, M.A. Atieh, T. Al-Ansari, Kinetic and thermodynamic investigations of surfactants adsorption from water by carbide-derived carbon, J. Environ. Sci. Health, Part A, 56 (2021) 1206–1220.

[S12] M.A. Khan, M.I. Khan, S. Zafar, Removal of different anionic dyes from aqueous solution by anion exchange membrane, Membr. Water Treat., 8 (2017) 259–277.

[S13] M.I. Khan, S. Akhtar, S. Zafar, A. Shaheen, M.A. Khan, R. Luque, Removal of Congo red from aqueous solution by anion exchange membrane (EBTAC): adsorption kinetics and themodynamics, Materials, 8 (2015) 4147–4161.

[S14] L. Liu, Y. Lin, Y. Liu, H. Zhu, Q. He, Removal of Methylene blue from aqueous solutions by sewage sludge based granular activated carbon: adsorption equilibrium, kinetics, and thermodynamics, J. Chem. Eng. Data, 58 (2013) 2248–2253.

[S15] M.I. Khan, J. Su, L. Guo, Development of triethanolamine functionalized-anion exchange membrane for adsorptive removal of methyl orange from aqueous solution, Desal. Water Treat., 209 (2021) 342–352.